Magneto-Optical Studies of Excited States of the Cl Donor in CdS

C. H. Henry and K. Nassau

Bell Telephone Laboratories, Murray Hill, New Jersey 07974
(Received 5 February 1970)

We have studied the $2s$ and $2p$ levels of the Cl donor in CdS by two methods: first, by observing "two-electron transitions" in which an exciton bound to the neutral donor Cl decays, leaving the donor in its $n = 2$ excited states; second, by observing Raman-scattering transitions between the $n = 1$ and $n = 2$ donor levels. We have accurately measured the positions of the $2p_x$, $2p_z$, and $2s$ levels relative to the $1s$ state to be 24.36 ± 0.02, 24.19 ± 0.02, and 23.88 ± 0.02 meV; the anisotropy factor $\alpha = 0.054 \pm 0.005$; and the electron mass $m_\perp = 0.190 \pm 0.002$. With less precision, we have measured $m_{\parallel} = 0.180 \pm 0.010$ and estimated the donor binding energy to be 32.7 ± 0.4 meV.

I. INTRODUCTION

Until recently, the primary means of studying excited states of shallow donors and acceptors has been by infrared absorption. These studies were primarily carried out in Si and Ge.[1] These materials were ideal because large single crystals, necessary for infrared studies, could be obtained and because there is no infrared absorption by the lattice in these homopolar materials. Other semiconductors of current interest, such as GaP and CdS, are infrared active and available only as small single crystals of high quality. Donors and acceptors in these materials are often more easily studied by other means which make use of visible spectroscopy. In recent years three techniques have emerged. The first technique is the analysis of donor-acceptor pair-recombination line spectra, which has been applied most extensively to GaP by Thomas *et al.*[2-5] The second technique involves two-electron transitions in which an exciton bound to a neutral donor decays, leaving the donor in an excited state. These transitions were first observed by Dean *et al.*[6,7] in GaP and Si and recently by Reynolds *et al.* in CdS,[8] CdSe,[9] and ZnO.[10] The third technique is electronic Raman scattering in which laser light scatters inelastically in a crystal, leaving a donor or acceptor in an excited state. These transitions have been observed by Henry *et al.*[11] and by Wright and Mooradian,[12] but thus far have provided little useful information about donors and acceptors.

In this paper, we have carefully repeated an experiment first carried out by Reynolds, Litton, and Collins (RLC)[8] in which they observed the decay of an exciton bound to a neutral donor in CdS. They observed a number of transitions in which the donor was left in several different excited states. We have observed these same two-electron transitions. In addition, we have observed electronic Raman-scattering transitions in which the donor is left in the same excited final states

that it is left in by the two-electron transitions.

RLC concluded from their analysis of the two-electron transition that the binding energy of a donor in CdS is about 26 meV. Previously, Hopfield and Thomas[13] had measured the binding energy of the A exciton in CdS to be 29.8 meV. The effective-mass binding energy of the donor should be greater than the effective-mass binding energy of the free exciton. This is because the donor binding energy is proportional to the electron effective mass, while the exciton binding energy is proportional to the reduced effective mass of the electron and hole. The result of RLC disagreed with this conclusion and it was this discrepancy that led us to repeat their measurements. We found that RLC overlooked the fact that some of the two-electron transitions arise from the decay of excited states of the bound exciton complex. Our analysis yields a binding energy of 32.7 ± 0.4 for the Cl donor. We are also able to precisely determine the $n = 1$ to $n = 2$ transition energies of the donor, the electron mass $m_\perp$, the anisotropy factor $(1 - m_\perp \epsilon_\perp / m_{\parallel} \epsilon_{\parallel})$, and make an approximate determination of $m_{\parallel}$.

Section II deals with experimental details. In Sec. III we discuss the effective-mass theory of the donor energy levels. Section IV deals with the observed transitions in zero magnetic field. Section V covers the Zeeman splittings of these transitions. In Sec. VI we estimate the donor binding energy. Finally, in Sec. VII we summarize our results and tabulate the values measured in this paper.

II. EXPERIMENTAL

A. Sample Preparation

Clear observation of the donor excited states requires a sample lightly doped with donors. Our crystals were platelets grown by sublimation in a flowing system. Our undoped crystals usually exhibited several I_2 lines,[14] indicating that there were

several prominent donors. By growing crystals in a system that had been contaminated with HCl vapor, we were able to obtain crystals that were lightly doped and had a single I_2 line due to the Cl donor. These crystals also had an I_1 line about as strong as the I_2 line. Luminescence associated with the I_1 line interfered with the observation of some of the two-electron transitions. We were able to reduce the intensity of the I_1 line by several orders of magnitude by sealing these crystals in a small quartz ampoule containing Cd metal and annealing them at 500 °C for 30 min. The reduction of the I_1 line by annealing in Cd vapor had previously been demonstrated by Handelman and Thomas.[15]

B. Spectroscopy

The luminescence and Raman scattering were observed photographically using a 2-m focal-length Bausch and Lomb spectrograph. The energy spectrum was calibrated with an iron-neon lamp. The linewidths of the two-electron transitions were about 0.08 meV, and the resolution of the spectrograph was about 0.02 meV. Luminescence was excited using the 4765-Å line of an argon ion laser with an intensity of about 40 mW focused. The Raman scattering was observed using the 4880-Å line of the argon laser with an intensity of about 200 mW focused. All measurements were made with the sample immersed in liquid helium pumped to 1.6 °K.

III. THEORY

A. Energy Levels

The theory of the energy levels and magnetic splitting of an exciton in a slightly anisotropic crystal was worked out by Hopfield and Thomas[13] and by Wheeler and Dimmock.[16] These theories apply equally well to a donor in CdS. We will use the notation of Wheeler and Dimmock.[16]

The effective-mass Hamiltonian for the donor electron at the zone center in a uniaxial crystal, with the c axis along the z direction, is given by[16]

$$H = \frac{[\vec{p}_\perp(e/c)\vec{A}_\perp]^2}{2m_\perp m_e} + \frac{[p_z + (e/c)A_z]^2}{2m_\parallel m_e}$$
$$- \frac{e^2}{\epsilon_0(x^2+y^2+z^2\epsilon_\perp/\epsilon_\parallel)^{1/2}}$$
$$+ g_\perp\beta\vec{H}_\perp \cdot \vec{S}_\perp + g_\parallel\beta H_z S_z \quad , \tag{1}$$

where

$$\vec{A} = \tfrac{1}{2}(\vec{H}\times\vec{r}), \quad \beta = e\hbar/2m_e c, \quad \epsilon_0 = (\epsilon_\perp\epsilon_\parallel)^{1/2} \quad . \tag{2}$$

Wheeler and Dimmock[16] make the coordinate transformation

$$(x,y,z) = [x', y', z'(m_\perp/m_\parallel)^{1/2}] \quad . \tag{3}$$

In this coordinate system the nonmagnetic part of the Hamiltonian simplifies to

$$\mathcal{3C} = \vec{p}'^2/2m_e m_\perp - e^2/\epsilon_0 r' + \mathcal{3C}_\alpha \quad , \tag{4}$$

where

$$\mathcal{3C}_\alpha = -(e^2/\epsilon_0)\{[x'^2+y'^2+z'^2(1-\alpha)]^{-1/2} - r'^{-1}\} \quad ,$$
$$\alpha = 1 - \epsilon_\perp m_\perp/\epsilon_\parallel m_\parallel \quad . \tag{5}$$

$\mathcal{3C}_\alpha$ is a small perturbation, when the anisotropy factor α is small. For $\alpha = 0$, the donor energy levels in zero magnetic field are hydrogenic. The donor binding energy for $\alpha = 0$ is given by

$$E_0 = E_H m_\perp/\epsilon_{0\perp}\epsilon_{0\parallel} \quad , \tag{6}$$

where E_H is the hydrogen atom binding energy. Using first-order perturbation theory, Wheeler and Dimmock calculate the donor energy levels, for a magnetic field in the z direction, to be

$$E_{1s} = -E_0(1+\tfrac{1}{3}\alpha+\tfrac{1}{20}\alpha^2) + \sigma H_z^2 \pm \tfrac{1}{2}g_\parallel\beta H_z \quad ,$$
$$E_{2s} = -\tfrac{1}{4}E_0(1+\tfrac{1}{3}\alpha+\tfrac{1}{20}\alpha^2) + 14\sigma H_z^2 \pm \tfrac{1}{2}g_\parallel\beta H_z \quad ,$$
$$E_{2p_z} = -\tfrac{1}{4}E_0(1+\tfrac{3}{5}\alpha+\tfrac{9}{28}\alpha^2) + 6\sigma_z^2 \pm \tfrac{1}{2}g_\parallel\beta H_z \quad , \tag{7}$$
$$E_{2p_x} = E_{2p_y} = -\tfrac{1}{4}E_0(1+\tfrac{1}{5}\alpha+\tfrac{9}{140}\alpha^2)$$
$$+ 12\sigma H_z^2 \pm \tfrac{1}{2}g_\parallel\beta H_z \pm \beta H/m_\perp \quad ,$$

where σ, the constant determining the diamagnetic shift, is given by

$$\sigma = \beta^2/2m_\perp^2 E_0 \quad . \tag{8}$$

When the magnetic field is in the x direction ($H\perp$ c axis), the eigenvalues are

$$E_{1s} = -E_0(1+\tfrac{1}{3}\alpha+\tfrac{3}{20}\alpha^2) + \sigma(m_\perp/m_\parallel)H_x^2 \pm \tfrac{1}{2}g_\perp\beta H_x \quad ,$$
$$E_{2s} = -\tfrac{1}{4}E_0(1+\tfrac{1}{3}\alpha+\tfrac{3}{20}\alpha^2)$$
$$+ 14\sigma(m_\perp/m_\parallel)H_x^2 \pm \tfrac{1}{2}g_\perp\beta H_x \quad ,$$
$$E_{2p_x} = -\tfrac{1}{4}E_0(1+\tfrac{1}{5}\alpha+\tfrac{9}{140}\alpha^2)$$
$$+ 6\sigma(m_\perp/m_\parallel)H_x^2 \pm \tfrac{1}{2}g_\perp\beta H_x \quad . \tag{9}$$

The states $2p_y$ and $2p_z$ are coupled by the magnetic field. The energies of these states are

$$\begin{Bmatrix} E_{2p_y} \\ E_{2p_z} \end{Bmatrix} = -\tfrac{1}{4}E_0(1+\tfrac{2}{5}\alpha+\tfrac{27}{140}\alpha^2) + 12\sigma(m_\perp/m_\parallel)H_x^2$$
$$\pm [(\tfrac{1}{2}\Delta)^2 + \beta^2 H_x^2/m_\perp m_\parallel]^{1/2} \pm \tfrac{1}{2}g_\perp\beta H_x \quad , \tag{10}$$
$$\Delta = \tfrac{1}{4}E_0(\tfrac{2}{5}\alpha+\tfrac{9}{35}\alpha^2) \quad .$$

B. Transition Probabilities

In the effective-mass approximation, the donor wave function is given by an envelope function $\varphi_D(\vec{r})$ multiplied by a zone center electron Bloch function. Similarly, the bound exciton complex, consisting of two electrons and a hole, can be written as a product of an envelope function $\varphi(\vec{r}_1, \vec{r}_2, \vec{r}_v)$ and three Bloch functions corresponding to the two

electrons and a hole with coordinates $\vec{r}_1$, $\vec{r}_2$, and $\vec{r}_v$. While the crystal itself does not have inversion symmetry, the effective-mass Hamiltonian is invariant under inversion of all the position coordinates. Therefore, the envelope functions will have a definite parity. The transition probability for the decay of the exciton will be proportional to the square of the overlap integral

$$\int \int \varphi_D(\vec{r}_1)^* \varphi(\vec{r}_1, \vec{r}_v, \vec{r}_v) e^{i\vec{q} \cdot \vec{r}_v} d\vec{r}_1 d\vec{r}_v$$

$$\approx \int \int \varphi_D(\vec{r}_1)^* \varphi(\vec{r}_1, \vec{r}_v, \vec{r}_v) d\vec{r}_1 d\vec{r}_v + i\vec{q}$$

$$\cdot \int \int \varphi_D(\vec{r}_1)^* \varphi(\vec{r}_1, \vec{r}_v, \vec{r}_v) \vec{r}_v d\vec{r}_1 d\vec{r}_v \,, \qquad (11)$$

where $\vec{q}$ is the wave vector of the emitted photon. The first term on the right-hand side of Eq. (11) gives rise to allowed transitions such as the I_2 line, in which the donor is left in its $1s$ ground state, and the strongest two-electron transition, in which the donor is left in the $2s$ state. The second term on the right-hand side of Eq. (11) results in parity forbidden transitions which become observable due to the finite wave vector of the emitted photon; e.g., a two-electron transition to the $2p_x$ donor state, which is observable when the light is emitted in the x direction.

The ground state of the bound exciton complex can be regarded as having one electron bound to the donor in approximately a $1s$ orbital and the other electron as bound to the hole as an exciton. We have shown previously that this approximation gives a good value for the lifetime of the I_2 line.[17] In this approximation we would also expect the allowed transition to the $1s$ donor state (the I_2 line)

to be much greater than the transitions to the $2s$ donor state (two-electron transition), which is what is observed.

An exciton bound to a neutral donor is a three-particle complex consisting of two electrons and a hole. The excited states of this complex are very difficult to calculate and at present there is no published theory of these excited states analogous to the theory of Sec. III A for the excited states of a neutral donor. Hopfield[18] treated the ground state of the bound exciton complex in the approximation that the hole is very heavy compared to the electron. In this approximation the bound exciton complex is analogous to a H_2 molecule. Recently, Reynolds, Litton, and Collins[19] have used this model to calculate the lowest-lying $(2s_\sigma)$ excited electronic state of this complex. The state has an energy of about 17 meV above the ground state of the complex in agreement with their observations. The excited states we observe lie only a few meV above the ground state of the complex. These low-lying states are likely to be more analogous to the vibrational or rotational states of the H_2 molecule than to be analogous to electronic excited states. In this paper we are concerned only with the excited states of the donor and we will not attempt to identify the excited states of the bound exciton complex.

IV. SPECTRA IN ZERO MAGNETIC FIELD

A densitometer trace showing the transitions that we observe in zero magnetic field is shown in Fig. 1. Figure 2 is a level diagram showing
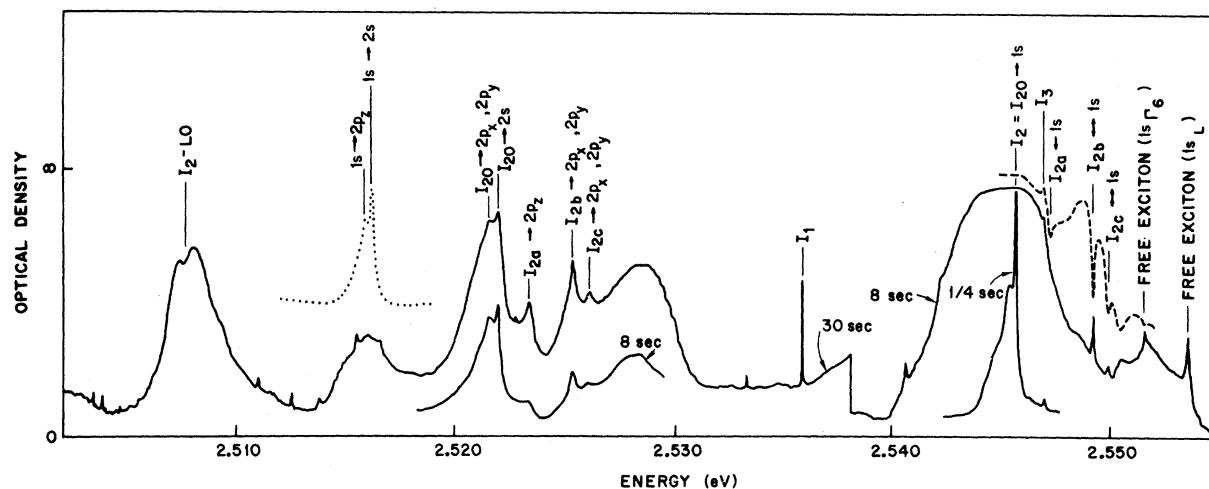

FIG. 1. Densitometer trace showing all bound exciton transitions and the Raman-scattering transitions in zero magnetic field. The I_2 line is labeled $I_{20} \rightarrow 1s$. The solid curve is luminescence for $\vec{q}_\perp c$ excited with 4765-Å argon laser light. The dashed curve shows the transitions from the $1s$ donor state to excited states of the bound exciton. These transitions are observed by the absorption of background luminescence. The dotted curve shows the Raman-scattering transitions and two-electron transitions for $\vec{q} \parallel c$, excited using 4880-Å argon laser light.
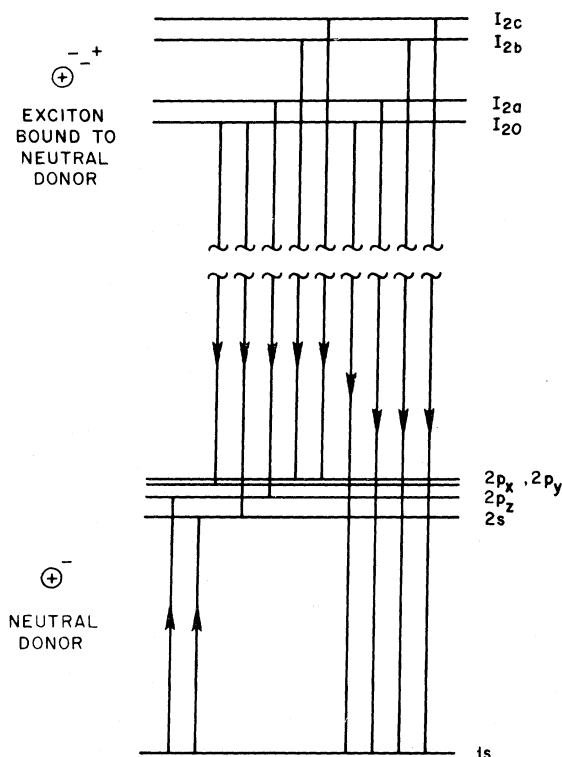
FIG. 2. Energy level diagram showing the transitions in Fig. 1. These transitions are in the same order from left to right as in Fig. 1.

the eleven transitions that occur in Fig. 1. The transitions in the level diagram are drawn from left to right in the same order as they occur in Fig. 1. The ground state of the bound exciton complex is labeled I_{20}. The three excited states of the bound exciton complex are labeled I_{2a}, I_{2b}, and I_{2c}. The donor levels are labeled $1s$, $2s$, $2p_x$, $2p_y$, $2p_z$. The structured peak near 2.5075 eV in Fig. 1 is the longitudinal optical-phonon replica of the I_2 line. In the remainder of this paper, the energies are measured relative to the I_2 line of the Cl donor. This line has an energy of 2.545 48 eV and an air wave length of 4869.12 Å.

A. Transitions to Donor Ground State

We were able to observe transitions from I_{2b} and I_{2c} to $1s$ in emission with $\vec{q} \perp c$. We were also able to observe the transitions of all three exciton excited states to $1s$ in absorption. This was done by observing luminescence along the thin edge of the platelet and exciting the luminescence along the side of the platelet. There was a broad background luminescence above the I_2 line which showed sharp absorption lines at energies corresponding

to the creation of the bound exciton complex in an excited state. It is not clear what the direction of $\vec{q}$ was for these transitions when the light was absorbed. From these transitions, we conclude that the energies of the excited states of the bound exciton complex are

$$E_{I_{2a}} = 1.66 \pm 0.02 \text{ meV} ,$$

$$E_{I_{2b}} = 3.77 \pm 0.02 \text{ meV} ,$$

$$E_{I_{2c}} = 4.49 \pm 0.02 \text{ meV} .$$

B. Transitions to Donor Excited States

The donor states were identified by their magnetic behavior. These first three transitions $I_{20} \to 2s$, $I_{20} \to 2p_x$, $2p_y$, and $I2a \to 2p_z$ allowed us to determine the energies of the donor levels above the donor ground state. These are

$$E_{2s} - E_{1s} = 23.88 \pm 0.02 \text{ meV} ,$$

$$E_{2p_z} - E_{1s} = 24.19 \pm 0.02 \text{ meV} ,$$

$$E_{2p_x} - E_{1s} = E_{2p_y} - E_{1s} = 24.36 \pm 0.02 \text{ meV} .$$

The positions of the other two transitions, $I_{2b} \to 2p_x$, $2p_y$ and $I_{2c} \to 2p_x$, $2p_y$ could be accurately predicted from the above parameters. The transition $I_{20} \to 2p_x$, $2p_y$ could not be seen for $\vec{q}_\parallel c$, as expected.

C. Raman-Scattering Transitions

We were also able to observe Raman-scattering transitions $1s \to 2s$ and $1s \to 2p_z$ as shown by the dotted curve in Fig. 1. The latter transition was observed in a geometry in which the light both entered the crystal and was backscattered along the c axis ($\vec{q}_\parallel z$). In this geometry, the laser beam had a long path length in the platelet. This was the only geometry convenient for observing Raman scattering in our apparatus. The Raman scattering confirmed our previous measurement of $E_{2s} - E_{1s}$ and $E_{2p_z} - E_{2s}$. This is the first observation of these Raman-scattering transitions. Previously, Thomas and Hopfield had observed donor Raman scattering of the form $1s$ (spin up) $\to 1s$ (spin down). [20]

V. ZEEMAN SPLITTINGS

All the transitions in Figs. 1 and 2 were split in a magnetic field, varied from 0 to 30.5 kG, for the two directions $\vec{H} \perp c$ and $\vec{H} \parallel c$. The splittings of the two-electron transitions become quite complicated, especially for $\vec{H} \perp c$. Small diamagnetic shifts of the states of the donor complex, the mixing of the $2s$ and $2p$ levels by the magnetic field, and the magnetic coupling of $n = 2$ states with higher donor levels have been neglected in calculating the theoretical curves. While the fit between theory and experiment is not perfect, it is quite adequate to identify unambiguously all of the transitions

shown in Fig. 1.

A. Splittings of Excited States of Bound Exciton Complex

The magnetic splittings of the transitions in which the bound exciton complex decays to the $1s$ state are shown in Fig. 3 for $\vec{H} \parallel c$ and Fig. 4 for $\vec{H} \perp c$. For $\vec{H} \parallel c$ the splittings are

$$g_\parallel (I_{20} \rightarrow 1s) = 0.00, \quad g_\parallel (I_{2a} \rightarrow 1s) = 0.54 ,$$

$$g_\parallel (I_{2b} \rightarrow 1s) = 1.30, \quad g_\parallel (I_{2c} \rightarrow 1s) = 0.82 .$$

Thomas and Hopfield showed that the I_2 line $(I_{20} \rightarrow 1s)$ does not split because the unpaired hole in the excited state accidentally has the same magnetic splitting for $\vec{H} \parallel c$, as the donor electron. We show no data in Fig. 3 for $I_{2a} \rightarrow 1s$. The small g value we assign to this level was inferred from the broadening of the $I_{2a} \rightarrow 2p_z$ transition with magnetic field.

For $\vec{H} \perp c$, transitions $I_{2a} \rightarrow 1s$ and $I_{2c} \rightarrow 1s$ split like $I_{20} \rightarrow 1s$, with the g value of the donor electron. We assume that, for these states of the bound exciton, the electron spins are paired off and the g value of the hole goes to zero for $\vec{H} \perp c$. The I_{2b} level of the complex is more complicated. The $I_{2b} \rightarrow 1s$ transition splits like $g_e \pm g(I_{2b})_\perp$, where $g_e = 1.75$ is the g value of the down electron. This indicates that unlike the other levels I_{2a} and I_{2c}, the I_{2b} level has a splitting for $\vec{H} \perp c$ with a g factor of

$$g_\perp (I_{2b}) = 1.15 .$$

Since the spin and orbital motion of the donor are uncoupled, we expect that g splittings of the transitions to the $1s$ state will be the same as the
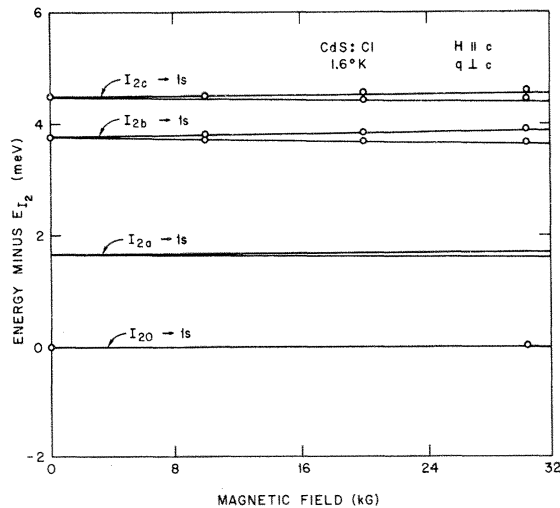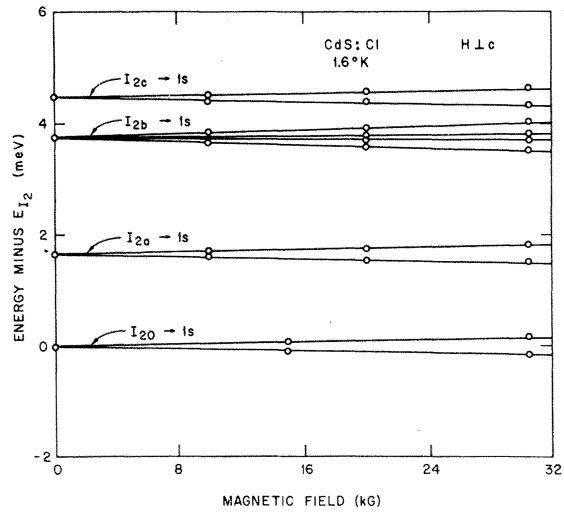

FIG. 4. Zeeman splittings of the bound exciton transitions to the $1s$ state for $\vec{H} \perp c$.

g splittings of the transitions to the $2s$ and $2p$ states. In the case of the $2p$ state we expect these splittings to add to the large splittings due to the orbital motion of the donor. This is exactly what is found. A striking example of this is the magnetic behavior of $I_{2b} \rightarrow 2p_x$, $2p_z$ transitions, shown later in Fig. 5, in which the splittings of the $I_{2b} \rightarrow 1s$ transition, shown in Fig. 4, are superimposed onto the larger orbital splittings of the $2p$ states. Another example of this is that for $\vec{H} \parallel c$, the $I_{20} \rightarrow 2s$ transition (Fig. 6) does not split just as the $I_{20} \rightarrow 1s$ transition (Fig. 3) does not split.

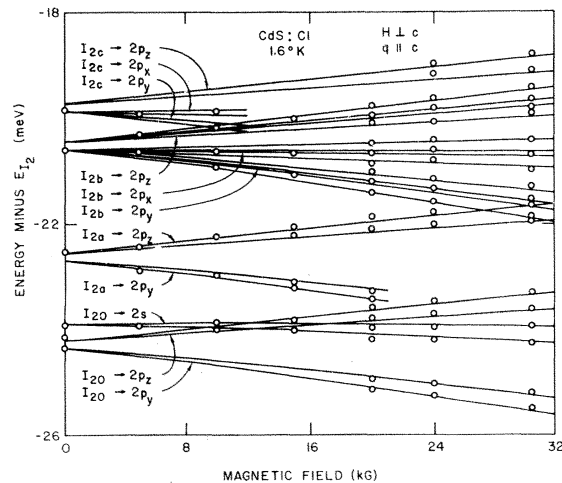FIG. 3. Zeeman splittings of the bound exciton transitions to the $1s$ state for $\vec{H} \parallel c$.

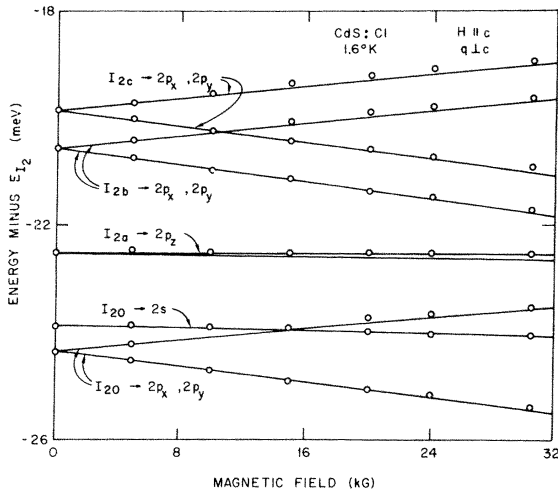FIG. 5. Zeeman splittings for the two-electron transitions from $\vec{H} \perp c$.

FIG. 6. Zeeman splittings of the two-electron transitions for $\vec{H} \parallel c$.

B. Magnetic Splittings of Two-Electron

Transitions

Figure 6 shows the splittings of the two-electron transitions for $\vec{H} \parallel c$, $\vec{q} \perp c$. The transition $I_{20} \to 2p_z$ is not observed. It is forbidden. The splittings of the $I_{20} \to 2p_x$, $2p_y$ correspond to a g factor of $2/m_\perp$. This allows us to accurately measure $m_\perp$ to be

$$m_\perp = 0.190 \pm 0.002 .$$

Using this value of $m_\perp$, the splittings of the $I_{2b} \to 2p_x$, $2p_y$ and $I_{2c} \to 2p_x$, $2p_y$ are fit quite well using g factors of $2/m_\perp + g_\parallel (I_{2b} \to 1s)$ and $2/m_\perp + g_\parallel (I_{2c} \to 1s)$.

The diamagnetic shift of the $I_{20} \to 2s$ transition is given by $13\sigma H^2 = 13(\beta H/m_\perp)^2/E_0$, assuming that the diamagnetic shift of the I_2 line is negligible. A value of

$$E_0 = 30.7 \pm 1.0 \text{ meV}$$

was used to fit this diamagnetic shift and also the diamagnetic shift of the $1s \to 2s$ transition observed in Raman scattering. The diamagnetic shifts are quite small and not a very sensitive measurement of E_0. In Sec. VI we calculate $E_0 = 33.0 \pm 0.4$ meV. Using the calculated value of E_0, we may calculate α from the separation of the $2p_z$ and $2p_x$ levels in zero field. We find that

$$\alpha = 1 - \epsilon_\perp m_\perp / \epsilon_\parallel m_\parallel = 0.050 \pm 0.005 .$$

Figure 5 shows the magnetic behavior of the two-electron transitions with $\vec{H} \perp c$, $\vec{q} \parallel c$. Because the spectrum is quite complicated, we have not plotted the transitions $I_{2c} \to 2p_x$, $I_{2c} \to 2p_y$, and

$I_{2a} \to 2p_y$ to high fields. These transitions were weak and could not be followed once they crossed stronger transitions. The transition $I_{20} \to 2p_x$ was forbidden and was not observed. The spin splittings of all the transitions are exactly the same as in the corresponding transitions to the $1s$ state shown in Fig. 4. The $2p_z$ and $2p_y$ levels are coupled by the magnetic field in the x direction. The separation of these levels is

$$2[(\tfrac{1}{2}\Delta)^2 + \beta^2 H_x^2/m_\perp m_\parallel]^{1/2} .$$

For large H, the separation is inversely proportional to the square root of $m_\parallel$. Since this splitting is not very sensitive to $m_\parallel$, we cannot pin down its value very precisely. We find the best fit is given by $m_\parallel = 0.180 \pm 0.010$.

C. Zeeman Splittings of Raman-Scattering

Transitions

Figures 7(a) and 7(b) show the Raman-scattering transitions for $\vec{H} \parallel c$ and $\vec{H} \perp c$. For $\vec{H} \parallel c$, the Raman-scattering transitions were observed by sending the laser light $\perp$ to the plane of a 25-μ-thick platelet of CdS. Because of the small path length of the laser light, the signals were small and only the stronger $1s \to 2s$ transition was observed. Only transitions in which the spin does not change its orientation are allowed for $\vec{H} \parallel c$. $\vec{H} \perp c$, $\vec{q} \parallel z$, the transitions $1s \to 2s$, $1s \to 2p_z$, and $1s \to 2p_y$ are observable. For each of these orbital transitions there are three lines corresponding to spin up $\to$ spin down, spin down $\to$ spin up, and
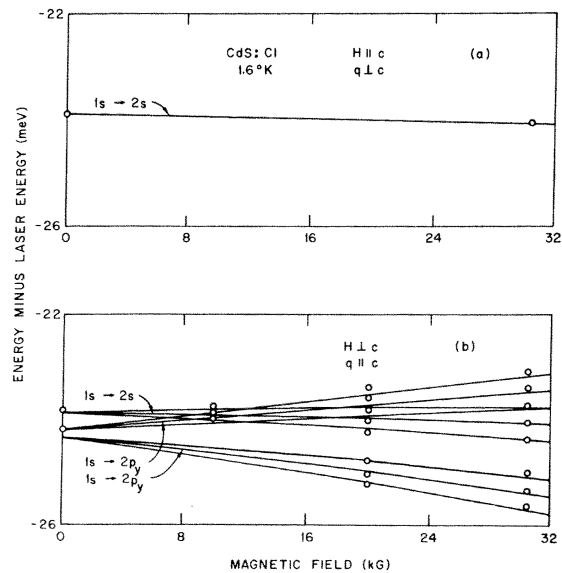

FIG. 7. Raman scattering transitions (a) $\vec{H} \parallel c$, $\vec{q} \perp c$, (b) $\vec{H} \perp c$, $\vec{q} \parallel c$.

spin unchanged.

VI. ESTIMATE OF DONOR BINDING ENERGY

We can estimate the binding energy of the Cl donor by adding the average binding energy of the $2p$ states to our measured average energy separation between $2p$ and $1s$ states. According to Eqs. (6) and (7), the average binding energy of the $2p$ states is

$$E_B(2p) = \tfrac{1}{4}(E_H m_\perp / \epsilon_{0\parallel} \epsilon_{0\perp})(1 + \tfrac{1}{3}\alpha + \tfrac{3}{20}\alpha^2). \quad (12)$$

The average energy separation of the $2p$ and $1s$ levels is 24.30 ± 0.02 meV. To evaluate Eq. (12) we can use our measured values of $m_\perp$ and α. Recently, Barker and Summers[21] have measured the static dielectric constants of CdS above the piezoelectric resonances. They find that $\epsilon_{0\perp} = 8.37 \pm 0.2$ and $\epsilon_{0\parallel} = 9.00 \pm 0.2$.

There will also be a contribution to the static dielectric constant due to screening by the acoustic phonons. The spherically averaged static dielectric constant ϵ, below the piezoelectric resonance, is given by

$$\epsilon = \epsilon_0 (1 + \langle K^2 \rangle) \,, \quad (13)$$

where ϵ_0 is the static dielectric constant above the piezoelectric resonance and $\langle K^2 \rangle$ is the squared electromechanical coupling constant spherically averaged over different directions of propagation. Hutson[22] has found that $\langle K^2 \rangle = 0.035$ for CdS. The screening of the Coulomb interaction by the acoustic phonons decreases the binding energy of Eq. (12) by a factor of $(1 + \langle K^2 \rangle)^{-2} \approx (1 - 2\langle K^2 \rangle)$. Actually, the screening is less than static screening, because the acoustic phonons can not follow the detailed motion of the electrons. Thus, we expect Eq. (8) to be decreased by a factor between unity and $(1 - 2\langle K^2 \rangle)$ by the screening of the Coulomb interaction by acoustic phonons. Evaluating Eq. (13) and taking into account this correction, we find that

$$E_B(2_p) = 8.4 \pm 0.4 \text{ meV}.$$

The errors take into account both the uncertainties in the measured dielectric constant and the uncertainties in the degree of screening by the acoustic phonons. Adding the average $2p$-$1s$ energy difference to this value gives us an estimate of the donor binding energy of

$$E_B = 32.7 \pm 0.4 \text{ meV}.$$

TABLE I. Summary of measured and estimated parameters.

$E_{2p_x} - E_{1s}$	24.36 $\pm$ 0.02 meV
$E_{2p_y} - E_{1s}$	24.36 $\pm$ 0.02 meV
$E_{2p_z} - E_{1s}$	24.19 $\pm$ 0.02 meV
$E_{2s} - E_{1s}$	23.88 $\pm$ 0.02 meV
$\alpha = 1 - m_\perp \epsilon_{\perp 0} / m_\parallel \epsilon_{\parallel 0}$	0.054 $\pm$ 0.005
$m_\perp$	0.190 $\pm$ 0.002
$m_\parallel$	0.180 $\pm$ 0.010
$E_{I_{2a}} - E_{I_{20}}$	1.66 $\pm$ 0.02 meV
$E_{I_{2b}} - E_{I_{20}}$	3.77 $\pm$ 0.02 meV
$E_{I_{2c}} - E_{I_{20}}$	4.49 $\pm$ 0.02 meV
E_B (estimate)	32.7 $\pm$ 0.4 meV

VII. SUMMARY

We have been able to observe transitions to the $n = 2$ donor states in CdS by two methods; by the decay of the bound exciton complex and by Raman scattering. The numerous transitions that we observed were unambiguously identified by their magnetic field splittings. The parameters that we have measured and estimated are tabulated in Table I. We have accurately measured the positions of the $2p_x$, $2p_z$, and $2s$ donor levels relative to the $1s$ ground state. We determined the anisotropy factor α from the splittings of the $2p$ levels. We also measured the positions of three excited states of the bound exciton complex. The nature of these states is not clear at present. From the magnetic field splittings we have obtained a precise measurement of $m_\perp$ and a less precise determination of $m_\parallel$. Our values for the electron masses are roughly 8.5% lower than those measured by Hopfield and Thomas[13] in their studies of the free exciton. They are also about 9.5% lower than the free-electron masses measured recently by Vella-Coleiro[23] from the Landau-level splittings.

Making use of our measured $2p$-$1s$ transition energies, our measured values of $m_\perp$ and α, and the static dielectric constants for CdS recently measured by Barker and Summers,[21] we have estimated the donor binding energy to be 32.7 ± 0.4 meV. This value agrees with the Hall studies of Piper and Halsted[24] which gave a binding energy of 32 ± 2 meV for donors in CdS.

[1]See, for example, R. L. Aggarwal, F. Fisher, V. Mourzive, and A. K. Ramdas, Phys. Rev. 138, A882 (1965).

[2]D. G. Thomas, M. Gershenzon, and F. A. Trumbore, Phys. Rev. 133, A269 (1964).

[3]F. A. Trumbore and D. G. Thomas, Phys. Rev. 137, 1030 (1965).

[4]P. J. Dean, C. H. Henry, and C. J. Frosch, Phys. Rev. 168, 812 (1968).

[5]P. J. Dean, C. J. Frosch, and C. H. Henry, J. Appl. Phys. 39, 5631 (1968).

[6]P. J. Dean, J. D. Cuthbert, D. G. Thomas, and R. T. Lynch, Phys. Rev. Letters 18, 122 (1967).

[7]P. J. Dean, J. R. Haynes, and W. F. Flood, Phys. Rev. 188, 711 (1969).

[8]D. C. Reynolds, C. W. Litton, and T. C. Collins, Phys. Rev. 174, 845 (1968).

[9]D. C. Reynolds, C. W. Litton, and T. C. Collins, Phys. Rev. 177, 1161 (1969).

[10]D. C. Reynolds and T. C. Collins, Phys. Rev. 185, 1099 (1969).

[11]C. H. Henry, J. J. Hopfield, and D. G. Thomas, Phys. Rev. 17, 1178 (1966).

[12]G. B. Wright and A. Mooradian, in Proceedings of the Ninth International Conference on the Physics of Semiconductors, edited by S. M. Ryvkin (Nauka, Leningrad,

1968), p. 1067; Phys. Rev. Letters 18, 608 (1967).

[13]J. J. Hopfield and D. G. Thomas, Phys. Rev. 122, 35 (1961).

[14]D. G. Thomas and J. J. Hopfield, Phys. Rev. 128, 2135 (1962).

[15]E. T. Handelman and D. G. Thomas, J. Phys. Chem. Solids 26, 1261 (1965).

[16]R. G. Wheeler and J. O. Dimmock, Phys. Rev. 125, 1805 (1962).

[17]C. H. Henry and K. Nassau, Phys. Rev. B 1, 1628 (1970).

[18]J. J. Hopfield, in Proceedings of the Seventh International Conference on the Physics of Semiconductors, Paris, 1964 (Academic, New York, 1965), p. 725.

[19]D. C. Reynolds, C. W. Litton, and T. C. Collins, Proc. Roy. Soc. (London) (to be published).

[20]D. G. Thomas and J. J. Hopfield, Phys. Rev. 175, 1021 (1968).

[21]A. S. Barker and C. J. Summers (unpublished).

[22]A. R. Hutson, J. Appl. Phys. Suppl. 32, 2287 (1961).

[23]G. Vella-Coleiro, Phys. Rev. Letters 23, 697 (1969).

[24]W. W. Piper and R. E. Halsted, in Proceedings of the International Conference on Semiconductor Physics, Prague, 1960 (Academic, New York, 1961), p. 1046.

Electric-Susceptibility Mass of Free Holes in SnTe[†]

R. F. Bis and J. R. Dixon

U.S. Naval Ordnance Laboratory, White Oak, Silver Spring, Maryland 20910

and

University of Maryland, College Park, Maryland 20740

The electric-susceptibility mass m_s of free carriers was determined at 300, 80, and 10 °K for p-type SnTe having carrier concentrations ranging from 3.6×10^{19} to 1.2×10^{21} cm^{-3}. The values were determined from an analysis of the normal reflectivity of the material in the infrared region. The observed carrier concentration and temperature dependences of m_s were used to test valence-band models recently proposed for SnTe by (i) Koehler, (ii) Rogers, and (iii) Tsu, Howard, and Esaki. In addition, a simple Cohen-type model was evaluated. It is demonstrated that none of these models provides a completely satisfactory description of our experimental results. The temperature dependence of m_s is shown to be anomalous with regard to its relationship to the temperature dependence of the forbidden energy gap. On the basis of our results, it is concluded that the valence-band structure of SnTe is considerably more complex than indicated by the models we have considered.

I. INTRODUCTION

Recently, a considerable amount of research has been directed toward an understanding of the valence-band structure of SnTe.[1-4] Despite this effort, the nature of this structure has not yet been delineated. Furthermore, a number of mutually inconsistent valence-band models have been proposed for this material.[2-4] An objective of the work which we report here was to test these band models by experimentally determining the electric-susceptibility mass m_s as a function of temperature and carrier concentration. Measurements of m_s are particularly useful for this purpose, because they are sensitive to the nature of the contributing bands at the Fermi level. Since the position of the Fermi level can be changed by varying the carrier concentration, various parts of the band